New Journal of Physics
The open access journal at the forefront of physics

Deutsche Physikalische Gesellschaft DPG IOP Institute of Physics

OPEN ACCESS

The two-electron attosecond streak camera for time-resolving intra-atomic collisions

To cite this article: A Emmanouilidou *et al* 2010 *New J. Phys.* **12** 103024

View the article online for updates and enhancements.

You may also like

- Study of attosecond delays using perturbation diagrams and exterior complex scaling
J M Dahlström and E Lindroth
- Attosecond laser station
Hao Teng, , Xin-Kui He et al.
- Attosecond technology(ies) and science
Jens Biegert, Francesca Calegari, Nirit Dudovich et al.

This content was downloaded from IP address 3.135.207.129 on 06/05/2024 at 14:41

New Journal of Physics
The open-access journal for physics

The two-electron attosecond streak camera for time-resolving intra-atomic collisions

A Emmanouilidou[1,2,4], A Staudte[3] and P B Corkum[3]

[1] Department of Physics and Astronomy, University College London, Gower Street, London WC1E 6BT, UK
[2] Chemistry Department, University of Massachusetts at Amherst, Amherst, MA 01003, USA
[3] Joint Laboratory for Attosecond Science, University of Ottawa and National Research Council, 100 Sussex Drive, Ottawa, ON, Canada, K1A 0R6
E-mail: a.emmanouilidou@ucl.ac.uk

New Journal of Physics **12** (2010) 103024 (8pp)
Received 6 August 2010
Published 14 October 2010
Online at http://www.njp.org/
doi:10.1088/1367-2630/12/10/103024

Abstract. We generalize the one-electron attosecond streak camera to time-resolve the correlated two-electron escape dynamics during a collision process involving a deep core electron. The collision process is triggered by an extreme ultraviolet (XUV) attosecond pulse (single-photon absorption) and probed by a weak infrared field. The principle of our two-electron streak camera is that by placing the maximum of the vector potential of the probing field at the time of collision, we get the maximum splitting of the inter-electronic angle of escape. We thereby determine the time of collision.

Differential measurements of fragmentation triggered by extreme ultraviolet (XUV) or x-ray single-photon absorption have been very successful in unraveling the multi-electron structure of atoms and molecules. The mechanisms of single photon break-up processes have been studied extensively in theory and experiment over the past two decades [1]. However, in conventional photo-ionization experiments, the initial and final states of the fragments are the only accessible observables. Attosecond technology, on the other hand, provides the tools to follow correlated particle dynamics in real time [2]. With the advent of laser pulses that last only a few tens of attoseconds [3], time-resolved measurements of inner shell dynamics have become conceivable [4].

[4] Author to whom any correspondence should be addressed.

© IOP Publishing Ltd and Deutsche Physikalische Gesellschaft

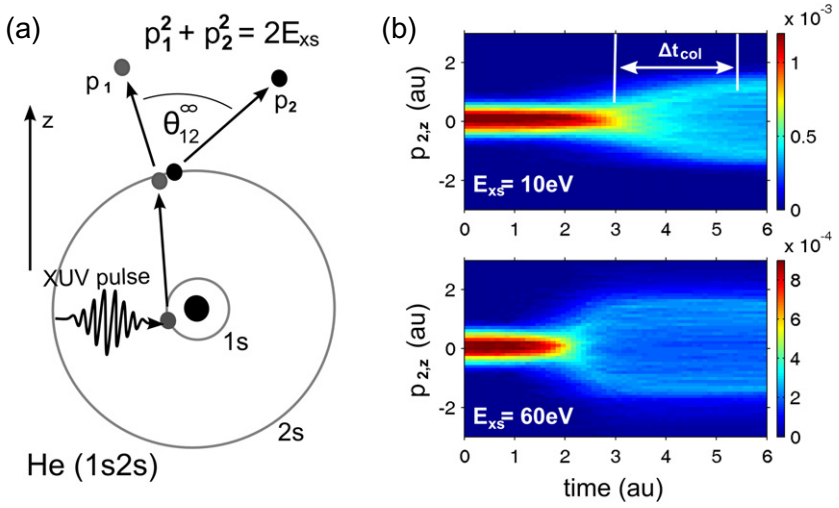

Figure 1. (a) A schematic picture of the collision triggered by an XUV pulse at time $t = 0$. (b) The probability density for the z momentum component for the 2s electron for 10 eV (top row) and 60 eV (bottom row) excess energy. The sudden change in momentum $\Delta t_{\rm col}$ takes place in the time interval between 3 and 5.5 au for 10 eV and 2 au and 3 au for 60 eV.

We generalize the attosecond streak camera [5] to two escaping electrons. Specifically, we formulate the concept for time-resolving the correlated electron dynamics in the knockout mechanism [6] (sometimes called 'two-step-one') with the primary electron knocking out the secondary electron in a (e, 2e)-like process.

In the one-electron streak camera [3]–[5], [7]–[9], the asymptotic electron momentum is modified by the instantaneous laser field at the time the electron is 'born' into the continuum. Measuring the distribution of the electron's final momentum, we determine the range for the electron's 'moment of birth'. One might expect that an analogous idea, applied to an observable that measures electronic correlation, can establish the range for the 'moment of intra-atomic collision'. Since the angle between the momenta of the escaping electrons—the inter-electronic angle θ_{12}—is an established observable for electronic correlation, we rely on θ_{12} for formulating the principle of the two-electron streak camera.

Figure 1(a) illustrates the concept of our two-electron streak camera, using as a model system the single-photon absorption from He(1s2s). First, the 1s electron absorbs an XUV photon with an energy above the double ionization threshold. Then, as the electron leaves the atom it can collide with the 2s electron and transfer some of its energy, resulting in the simultaneous ejection of both electrons. We will show that the inter-electronic angle θ_{12} provides details of the time scale of the intra-atomic e–e collision.

We choose He(1s2s) as a prototype system to clearly formulate the concept of streaking two-electron dynamics while avoiding the unnecessary complexity of many-electron systems. However, the scheme is not system specific. The same scheme could time-resolve, for instance, the collision between 1s and 2s electrons in the ground state of Li.

The probing in our two-electron streak camera is achieved by the presence of a weak optical field during the XUV absorption, with both pulses polarized in the same direction. In the absence of the streaking field the distribution of the inter-electronic angle θ_{12} peaks around

a well-defined value characteristic of the photon energy. When the streaking (probing) field is present, the observable θ_{12} decreases or increases depending on the direction the 1s electron is emitted with respect to the vector potential of the laser field. The amount of splitting to lower and higher values depends on the phase of the streaking field. (In the following, photo-electron refers to the electron that initially absorbs the XUV photon.) We measure the phase of the probing field with respect to the time the XUV attosecond pulse is applied. If we place the maximum of the vector potential at the time of collision, we get maximum splitting in θ_{12}. This allows us to identify a characteristic time for the collision.

To test the two-electron camera concept, we employ a three-dimensional classical trajectory Monte Carlo simulation [10]. Our model [11] assumes that the 1s electron absorbs the single photon at the nucleus [11]–[15]—an approximation that becomes exact in the high energy limit. The initial conditions for the secondary electron (2s) are generated using the Wigner distribution [16] of the 2s hydrogenic orbital restricted on an energy shell. The energy shell corresponds to the ionization energy needed to remove the 2s electron from He(1s2s) [13]. To avoid problems associated with electron trajectories starting at the nucleus we use regularized coordinates [17]. Our propagation scheme fully accounts for all interactions with no approximations. Previous studies applying this approach on full break-up of three electrons were found to be in very good agreement with experimental and quantum mechanical results from the threshold up to intermediate excess photon energies—see [11, 14, 15]. Quasiclassical techniques have been critical for demonstrating that single-photon break-up of three-electron atoms occurs via a sequence of two attosecond collisions [13].

Today's shortest available XUV pulses of 80 as [3] have a bandwidth of >20 eV. A transform-limited, Gaussian pulse with 10 as duration would have a bandwidth of >180 eV. The two-electron streak camera also operates for these broadband pulses, since in the experiment the photon energy for each event can be easily determined *a posteriori* from the sum of the electron momenta. Hence, it is not necessary to simulate photoelectron energies corresponding to the bandwidth of real attosecond pulses, and we will restrict our model to two discrete photon energies to illustrate the difference in ionization timescales for different photon energies. In the experiment, measuring θ_{12} as a function of the photon energy will provide the complete picture of the attosecond intra-atomic collision, in analogy to frequency resolved optical gating (FROG) commonly used to characterize femtosecond pulses [18].

In figure 1(b) we show the classical probability density of the z momentum components for the 2s electron for excess photon energies, E_{xs}, of 10 eV/60 eV, where $E_{xs} = E_{XUV} - Ip$ and Ip is the fragmentation energy of He(1s2s). The (e,2e) collision, sketched in figure 1(a), is clearly traced in the classical probability densities (see [13])—the closest analogue to a quantum mechanical density. A sudden momentum change as a signature of the collision occurs approximately between $t = 3$–5.5 au/$t = 2$–3 au for 10 eV/60 eV excess energy. The transfer of momentum happens much faster with increasing excess energy, resulting in an earlier time of collision. We show that the two-electron streak camera measures the time, t_{col}, when the sudden momentum change is complete.

The collision between the two electrons is also visible in figure 2 when plotting the probability density for θ_{12} for 10 eV and 60 eV excess energies. The sudden increase in θ_{12} as the two electrons move away from each other and escape from the nucleus is a signature of the two-electron collision. For the higher excess energy, the change in θ_{12} takes place earlier and over the same time interval as the change in momentum (figure 1). For very large times, θ_{12} reaches the asymptotic value of $\theta_{12}^{\infty} = 135^{\circ}/105^{\circ}$ for 10 eV/60 eV. Comparing figures 1 and 2 we

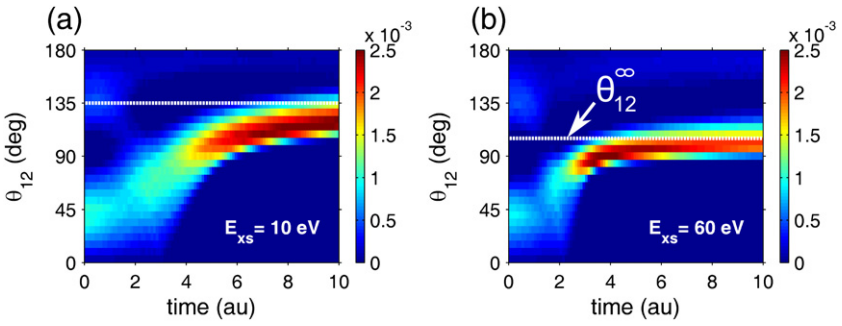

Figure 2. Probability density of θ_{12} as a function of time for photon excess energy of 10 eV (a) and 60 eV (b). The sudden change in θ_{12} takes place in the time interval between 3 and 5.5 au for 10 eV and between 2 and 3 au for 60 eV. $t_{\rm col} \approx 5.5$ au/3 au for 10 eV/60 eV. At very large times, θ_{12} reaches the asymptotic value of $\theta_{12}^{\infty} = 135^{\circ}/105^{\circ}$ for 10 eV/60 eV, respectively.

see that θ_{12} is a much better observable for streaking than p_z because θ_{12} has a much narrower asymptotic distribution.

The electric field used to probe the two-electron collision is $\vec{E} = E_0 f(t)\cos(\omega t + \phi)\hat{z}$, where ω is the frequency, ϕ is the phase of the field and $f(t)$ is the pulse envelope. For our calculations we use $f(t) = 1$ for $0 < t < 2T$ and $f(t) = \cos^2((t-2T)\omega/8)$ for $2T < t < 4T$. Time zero corresponds to the time the photon is absorbed from the 1s electron. In the experiment, the time zero can be established in the single ionization channel using the conventional one-electron streak camera [3].

Introducing the weak infrared laser field has two ramifications for the calculation. First, it requires solving a non-conservative driven three-body Coulomb system, in contrast to the single photon process where the energy is conserved. Our propagation scheme has been generalized to account for laser-driven processes [19]. In addition, it breaks the spherical symmetry of the single-photon process. To account for the latter we slightly modify the initial phase space distribution along the lines of [20]—we take z to be the axis of polarization of the XUV pulse and weight the trajectories by a $\cos^2\theta_{p_{1s}}$ dipole distribution for the photo-electron.

We use a probing infrared pulse with frequency $\omega = 0.0285$ au (1600 nm) and strength $E_0 = 0.007$ au/0.009 au ($< 3 \times 10^{12}$ W/cm^2) for 10 eV/60 eV excess energy. E_0 and ω are not critical, except that the pulse should not significantly alter the attosecond collision and it must have an observable effect on θ_{12}. The streaking field that we use corresponds to a very small Ammosov–Delone–Krainov (ADK) tunneling rate [21] and so we ignore tunneling of the 2s electron. Even if tunneling were important, it could be separated from the double ionization process by the low kinetic energy of the above threshold ionization (ATI) electrons just as is done in the single-electron streak camera [7]–[9].

Depending on the phase of the streaking field, the probe pulse can have a major effect on the asymptotic angular spectrum of the two escaping electrons. As shown in figure 3(b), the probing pulse causes a clear splitting of the inter-electronic angle around $\theta_{12}^{\infty} = 135^{\circ}/105^{\circ}$ (see figure 2) for 10 eV/60 eV. The maximum split of θ_{12} occurs for a phase of the field $\phi_{\rm delay}$ that is smaller than $\phi_0 = 90^{\circ}$. (ϕ_0 is the phase corresponding to the maximum of the vector potential $A(\phi)$ at $t = 0$, where $-\frac{\partial \vec{A}(t)}{\partial t} = \vec{E}(t)$.) Extracting the relevant information from figure 3(b) (see below for how we do so) we find that $\Delta\phi = \phi_0 - \phi_{\rm delay} = 9^{\circ}/4.5^{\circ}$ corresponding to $t_{\rm col} = 5.5$ au/2.76 au

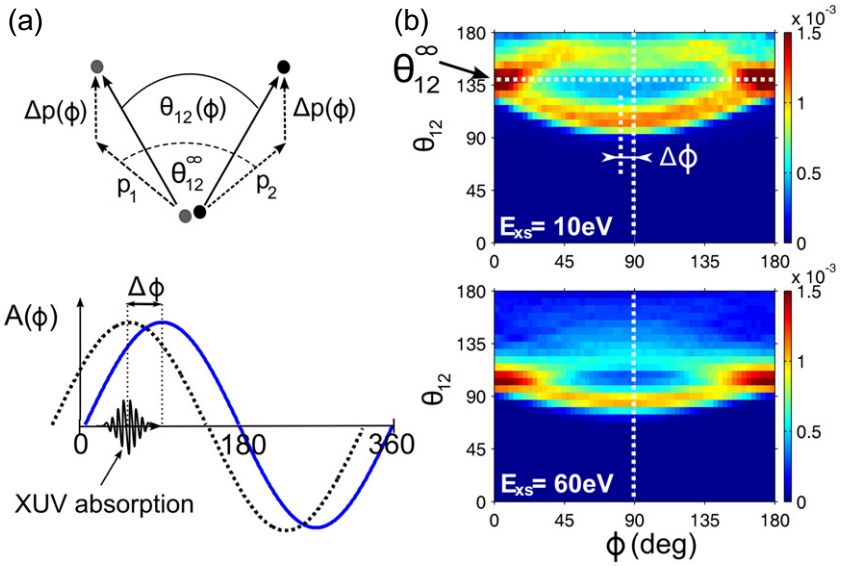

Figure 3. (a) The streaking field causes a decrease in θ_{12} when the photo-electron is launched along the $+\hat{z}$ direction, since adding Δp to each of the electron momenta results in $\theta_{12} < \theta_{12}^{\infty}$. (b) θ_{12} as a function of ϕ for 10 eV/60 eV (top/bottom row) excess energies in the presence of an XUV attosecond pulse and a weak infrared laser field. $\Delta\phi$ is the shift of the maximum of the vector potential, corresponding to a maximum of the split of θ_{12} as a function of ϕ. $\Delta\phi = 9^{\circ}/4.5^{\circ}$ for 10 eV/60 eV.

for 10 eV/60 eV. The collision times we determine from figure 3(b) agree with the collision times in figures 1 and 2 for both 10 and 60 eV excess energies.

We now develop an analytical model for the split of the inter-electronic angle of escape as a function of the phase of the field and to show why $\Delta\phi$ gives the collision time. A small change in the photo-electron momentum has a negligible impact on θ_{12}. Therefore, we can neglect the interaction between the weak streaking field and the photo-electron before the collision. In addition, we assume that the transfer of energy from the 1s to the 2s electron is sudden. Figures 1 and 2 show that this assumption is only approximately valid. Finally, we assume that the streaking pulse is zero at $t = \infty$. The change in momentum for each electron due to the streaking pulse is given by

$$\Delta\vec{p}(\phi, t_{\mathrm{col}}) = -\int_{t_0}^{\infty} \vec{E} = -E_0 \int_{t_{\mathrm{col}}}^{\infty} f(t)\cos(\omega t + \phi)\hat{z}$$

$$= \frac{E_0}{\omega}\sin(\omega t_{\mathrm{col}} + \phi)\hat{z} = -\vec{A}(\omega t_{\mathrm{col}} + \phi). \tag{1}$$

From equation (1) we see that the momentum change due to the streaking infrared field is along the positive $\hat{z}$-axis. Δp depends on t_{col} and the phase ϕ of the streaking field. Since $\Delta p > 0$, the effect of the streaking field on the doubly ionizing events is different depending on the initial direction of launching of the photo-electron. As shown in figure 3(a), if the photo-electron is launched along the positive $\hat{z}$-axis, then adding Δp to each of the electron momenta results in $\theta_{12} < \theta_{12}^{\infty}$, thus accounting for the lower split of θ_{12} in figure 3(b). Similarly, if the photo-electron is launched along the negative $\hat{z}$-axis, then subtracting Δp from each of the

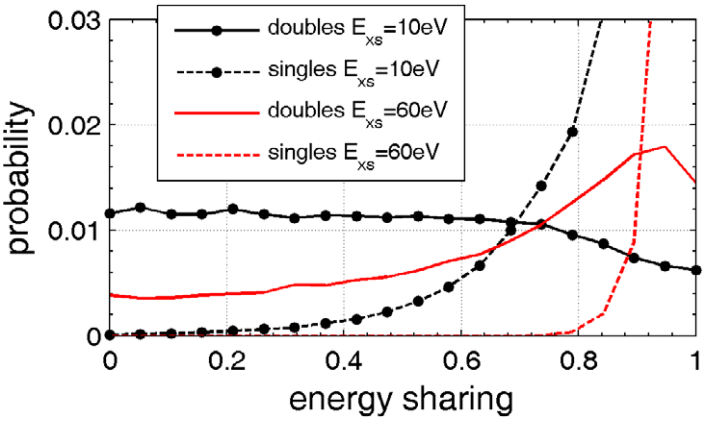

Figure 4. The double ionization probability as a function of energy sharing averaged over all phases ϕ when the streaking field is on separately for the 'double' and 'single' events for 10 eV/60 eV excess energy. The area under the 'double' events is 0.011/0.0084, whereas the area under the 'single' events is 0.013/0.0106. The sum of the two contributions is the total double ionization probability in the presence of the XUV attosecond pulse and the streaking field.

electron momenta results in $\theta_{12} > \theta_{12}^{\infty}$, thus accounting for the upper split of θ_{12} in figure 3(b). From equation (1) we also see that the maximum split in θ_{12} occurs at $\omega t_{\rm col} + \phi_{\rm delay} = 90^{\circ} = \phi_0$, resulting in $t_{\rm col} = \Delta\phi/\omega$.

In figure 3(b), our numerical results for θ_{12} are obtained including all final energy sharings between the two electrons. More asymmetric energy sharing corresponds to larger collision times. Many approaches work equally well for accurately determining $t_{\rm col}$. For example, one way is a simple fit of our numerical results for $\theta_{12}(\phi)$ in figure 3(b) with the analytic expression for θ_{12} that one obtains by adding $\Delta\vec{p}(\phi, t_{\rm col})$ to the final electron momenta (see figure 3(a)).

Our analytical model isolates the physics that underlies two-electron streaking. However, there remains another important issue. Classical physics has allowed us to select from all the trajectories that doubly ionize in the presence of the XUV and the streaking pulse only the trajectories that doubly ionize even in the absence of the streaking field (labeled below as 'doubles'). We now discuss how one can isolate experimentally the 'doubles'.

A small fraction of the events that singly ionize due to the XUV pulse involves the photoelectron exciting the 2s electron to Rydberg states. When the streaking field is subsequently turned on, it causes a fraction of the Rydberg states to ionize. We label the events that doubly ionize in the absence of the streaking field as 'double'. Events that doubly ionize only in the presence of the streaking field will be referred to as 'single'. The double ionization probability due to the XUV pulse alone is 0.011/0.0084 ('double' events). When the streaking field is turned on, the double ionization probability increases to 0.024/0.019 with 0.011/0.0084 contribution from the 'double' and 0.013/0.0106 from the 'single' events for 10 eV/60 eV. These numbers were obtained by averaging over all phases ϕ. There is a phase dependence of the double ionization probability of 'singles' and of their momentum distribution. Although not the focus of this paper, the 'singles' provide an observable that can be exploited to characterize the bound state electron wavepacket created by the internal two-electron collision.

'Single' trajectories can be separated from the 'doubles' if one considers the energy sharing, $\frac{|\epsilon_1-\epsilon_2|}{|\epsilon_1+\epsilon_2|}$, with ϵ_1, ϵ_2 being the asymptotic energies of the 1s and 2s electrons. Figure 4 shows that the 'single' trajectories typically have a high asymmetry in their energy sharing. In contrast, 'doubles' have a much smaller asymmetry. By considering only trajectories with asymmetry in energy sharing less than 0.85/0.95 in figure 4 for 10 eV/60 eV excess energy, we separate 64/70% of the 'singles' while losing only 9% of the 'double' events we want to probe. If, in addition, we use a cut-off in the inter-electronic angle, without further loss of 'double' events, we isolate 70/80% of the 'single' events. Both of these procedures for isolating the 'single' events are available to an experimentalist.

In conclusion, the two-electron streak camera can be applied to a large class of problems, i.e., the break-up by single-photon absorption of multi-electron atoms and molecules. These collision problems have been studied intensively during the last two decades [1]. It is well established that knockout is the mechanism that dominates for small and intermediate excess energies, whereas shakeoff dominates for large excess energies [22, 23]. The two mechanisms are usually separated by energy sharing [23]. The two-electron streak camera paves the way for time-resolving the knockout part of multi-electron collision processes triggered by a deep core electron after single-photon absorption. Time-resolving collisions in multi-electron systems are a problem at the forefront of attosecond science. So far, we have exploited only a fraction of the information available for the two-electron collision process. Further insight will be obtained by considering how the inter-electronic angle of escape depends on the energy sharing. Probing the electronic correlation for different energy sharing could lead to characterizing, to our knowledge for the first time, the single-photon break-up mechanisms by the timescales involved.

Acknowledgments

AE gratefully acknowledges funding from EPSRC (grant no. EPSRC/H0031771) and NSF (grant no. NSF/0855403) and thanks Jan Michael Rost and the Max Planck Institute for Complex Systems for access to their computational resources.

References

[1] Briggs J S and Schmidt V 2000 Differential cross sections for photo-double-ionization of the helium atom *J. Phys.* B **33** R1
[2] Corkum P B and Krausz F 2007 *Nat. Phys.* **3** 381
[3] Goulielmakis E *et al* 2008 Single-cycle nonlinear optics *Science* **320** 1614
[4] Drescher M, Hentschel M, Kienberger R, Uiberacker M, Yakovlev V, Scrinzi A, Westerwalbesloh Th, Kleineberg U, Heinzmann U and Krausz F 2002 Time-resolved atomic inner-shell spectroscopy *Nature* **419** 803
[5] Itatani J, Quéré F, Yudin G L, Ivanov M Yu, Krausz F and Corkum P B 2002 Attosecond streak camera *Phys. Rev. Lett.* **88** 173903
[6] Tanis J A *et al* 1999 Production of hollow lithium by multielectron correlation in 95 MeV/nucleon Ar^{18+} + Li collisions *Phys. Rev. Lett.* **83** 1131
[7] Drescher M, Hentschel M, Kienberger R, Tempea G, Spielmann Ch, Reider G A, Corkum P B and Krausz F 2001 X-ray pulses approaching the attosecond frontier *Science* **291** 1923
[8] Uiberacker M *et al* 2007 Attosecond real-time observation of electron tunnelling in atoms *Nature* **446** 627
[9] Eckle P, Pfeiffer A N, Cirelli C, Staudte A, Dörner R, Muller H G, Büttiker M and Keller U 2008 Attosecond ionization and tunneling delay time measurements in helium *Science* **322** 1525

[10] Abrines R and Percival I C 1966 *Proc. Phys. Soc.* **88** 861
[11] Emmanouilidou A and Rost J M 2006 *J. Phys.* B **39** 4037
[12] Schneider T, Chocian P L and Rost J M 2002 Separation and identification of dominant mechanisms in double photoionization *Phys. Rev. Lett.* **89** 073002
[13] Emmanouilidou A and Rost J M 2007 *Phys. Rev.* A **75** 022712
[14] Emmanouilidou A, Wang P and Rost J M 2008 Initial state dependence in multielectron threshold ionization of atoms *Phys. Rev. Lett.* **100** 063002
[15] Emmanouilidou A 2007 *Phys. Rev.* A **75** 042702
[16] Heller E J 1976 Wigner phase space method: analysis for semiclassical applications *J. Chem. Phys.* **65** 1289
[17] Kustaanheimo P and Stiefel E 1965 Multiphoton electron angular distributions from laser-aligned CS_2 molecules *J. Reine Angew. Math.* **218** 204
[18] Kane D J and Trebino R 1993 Characterization of arbitrary femtosecond pulses using frequency-resolved optical gating *IEEE J. Quantum Electron.* **29** 571
[19] Emmanouilidou A 2008 *Phys. Rev.* A **78** 023411
[20] Siedschlag Ch and Pattard T 2005 Single-photon double ionization of the hydrogen molecule *J. Phys.* B **38** 2297
[21] Delone N B and Krainov V P 1991 Energy and angular electron spectra for the tunnel ionization of atoms by strong low-frequency radiation *J. Opt. Soc. Am.* B **8** 1207
[22] Pattard T and Burgdörfer J 2001 Half-collision model for triple photoionization of lithium *Phys. Rev.* A **63** 020701
[23] Knapp A *et al* 2002 Mechanisms of photo double ionization of helium by 530 eV photons *Phys. Rev. Lett.* **89** 033004